

FRONTIER TECHNOLOGIES IN DESIGN AND CONSTRUCTION FOR SUSTAINABLE TRANSPORT INFRASTRUCTURE

Buddhima Indraratna,

Professor of Civil Engineering, and Director, Centre for Geomechanics & Railway Engineering
University of Wollongong, Australia
(email: indra@uow.edu.au)

Sanjay Nimbalkar,

Research Fellow, Centre for Geomechanics and Railway Engineering
University of Wollongong, Australia
(email: sanjayn@uow.edu.au)

Cholachat Rujikiatkamjorn,

Senior Lecturer, Centre for Geomechanics and Railway Engineering
University of Wollongong, Australia
(email: cholacha@uow.edu.au)

Abstract

Railways are expected to be one of the main modes of future transport in rapidly developing countries with high population densities, including Sri Lanka. In spite of recent advances in rail track geotechnology, ballasted tracks progressively degrade under heavy cyclic and impact loading. Field studies often provide significant knowledge to better understand track performance and to extend the current state-of-the-art in design. Therefore, comprehensive field trials were carried out on two instrumented rail tracks in Bulli and in Singleton, New South Wales, Australia. In these studies, several track sections were reinforced with different types of geosynthetics placed beneath the ballast embankment, with the aim of reducing track settlement, increasing track resiliency, and decreasing ballast degradation. The effects of impact loads and its mitigation using shock mats are discussed. A series of isotropically consolidated drained triaxial tests were conducted on both clean and clay-fouled ballast with varying fouling levels to establish the relationship between the extent of fouling and the associated strength-deformation properties. The outcomes of this research are now elucidated in view of industry practices. This keynote paper provides a fresh insight to design and performance of rail tracks capturing particle degradation, fouling and the use of geosynthetics in track design.

Keywords: Ballast, Degradation, Impact Loads, Fouling, Geosynthetics

1. Introduction

Rail Transport in Sri Lanka and Australia consists of a heavy rail network serving commuter and freight traffic. There is a great potential for expanding the freight rail system, but increasing the traffic tonnages and speed are limited by the conditions of the track and maintenance costs associated with its subsequent degradation. The large lateral deformations of ballast due to insufficient track confinement, fouling of ballast by coal from freight trains, unstable soft formation soils (clay pumping), ballast breakage under cyclic and impact loads are the primary causes of track deterioration. The complexities associated with the ballast are attributed to the effects of angularity, anisotropy, particle degradation, and in-situ confining pressure (Marshal, 1973; Indraratna et al., 1998, 2005, 2010a; Lackenby et al., 2007; Altuhafi and Coop, 2011), as well as the frequency of loading (Luo et al., 1996; Indraratna et al., 2011a; Nimbalkar et al. 2012a). Under cyclic loads, the cyclic densification of ballast and associated rail track deformations are important for the optimum design, safety, and operational efficiency of tracks.

Recently, few studies dealing with the adverse effects of fouling on the shear behaviour of ballast have been conducted (Tutumluer et al., 2008; Indraratna et al., 2012). When ballast is fouled by particle breakage or infiltration of coal or clay fines, the interlocking and frictional resistance reduces as fine particles clog the ballast voids. When the amount of fouling materials is excessive, fine particles can dominate the ballast behaviour and ultimately make the track unstable. The problem becomes more severe under impact loading that causes accelerated breakage of ballast, especially when the underlying formation soil is stiff. The amplitude and frequency of impact loads depend on the nature of wheel or rail irregularities as well as on the dynamic response of the rail track (Jenkins et al., 1974; Indraratna et al., 2011a). Installation of shock mats in rail tracks can attenuate these impact loads substantially.

The potential use of geosynthetics to improve track stability has been observed in several laboratory studies (Selig and Waters, 1994; Raymond, 2002; Indraratna and Salim, 2003; Indraratna and Nimbalkar, 2012). However, only a few studies have assessed the relative merits of geosynthetics and shock mats under in situ track conditions, while the in-situ performance of different types of geosynthetics to improve the overall stability of ballasted rail tracks has not been investigated in a systematic manner. Two extensive field studies are elaborated including the Bulli and Singleton sites where performances of various track sections were enhanced by synthetic grids and shock mats. This keynote paper describes the large-scale laboratory studies and full-scale field trials those advance the current state of the art knowledge in the geotechnical behaviour of ballast, including shear strength, particle breakage, ballast fouling and benefits of using geosynthetic grids and shock mats.

2. Extending the current state of the art

2.1 Ballast breakage

Railway tracks are severely affected by the degradation of ballast particles due to conventional cyclic and occasional high impact loads (Indraratna et al., 2011a,b). The particle breakage is a complex mechanism that usually starts at the inter-particle contacts (i.e. breakage of asperities), followed by a complete crushing of weaker particles under further loading. The breakage of ballast particles due to wheel loading can occur in three ways: (a) the breakage of particles into approximately equal pieces (particle splitting), (b) the breakage of angular projections and (c) the grinding off of small-scale asperities (Raymond and Diyaljee, 1979). Lackenby et al. (2007) showed that most ballast breakage is not attributable to particle splitting, but is instead primarily the consequence of the corner breakage. Indraratna et al. (2005) introduced a new Ballast Breakage Index (*BBI*) which is obtained on the basis of changes in the fraction passing a range of sieves, as shown in Figure 1. *BBI* can be calculated using the following equation.

$$BBI = \frac{A}{A+B} \quad (1)$$

where *A* is shift in the Particle Size Distribution (*PSD*) curve after the test, and *B* is the potential breakage or area between the arbitrary boundary of maximum breakage and the final particle size distribution. *BBI* has a lower limit of 0 (no breakage) and an upper limit of 1 (maximum breakage defined by an arbitrary boundary).

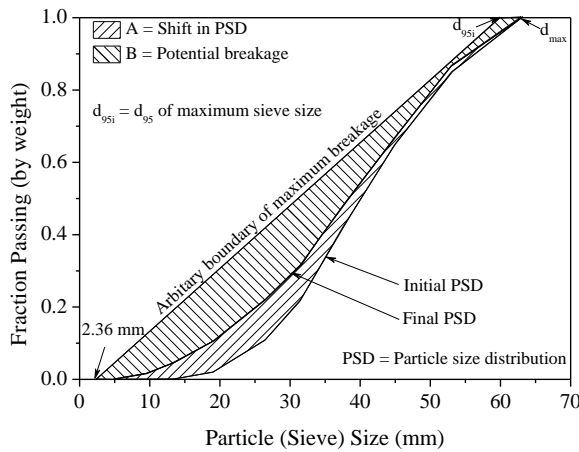


Figure 1: Ballast breakage index (*BBI*) calculation method (data sourced from Indraratna et al., 2005)

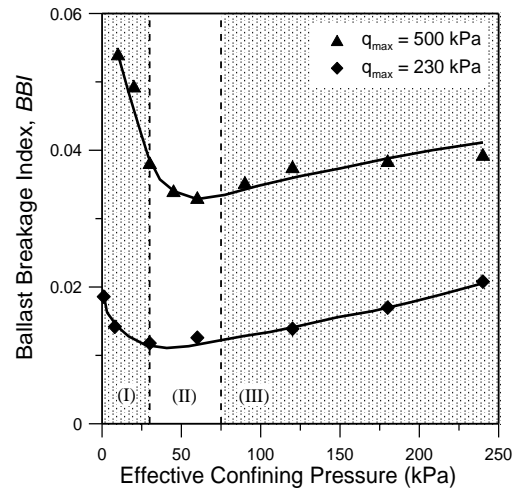


Figure 2: Effect of confining pressure on particle degradation (data sourced from Lackenby et al., 2007)

2.2 Confining pressure

Although the effect of confining pressure is significant, it is usually neglected in conventional design of the rail track. A series of cyclic triaxial tests were conducted to investigate the effect of confining pressure on ballast under cyclic loading (Lackenby et al., 2007). Specimens were prepared to the recommended gradation and initial porosity (i.e. $d_{50} = 38.5$ mm, $C_u = 1.54$, $e_o = 0.76$ where d_{50} is the diameter of the ballast corresponding to 50% finer in the particle size distribution curve, C_u is the coefficient of uniformity and e_o is initial void ratio). Effective confining pressures (σ_3') ranging from 1 to 240 kPa were applied. As shown in Figure 2, the degradation of ballast under cyclic loading is categorised into three distinct zones, namely: (I) the Dilatant Unstable Degradation Zone (*DUDZ*), (II) the Optimum Degradation Zone (*ODZ*), and (III) the Compressive Stable Degradation Zone (*CSDZ*). These zones are defined by the magnitude of confining pressure (σ_3') applied to the specimen (i.e. *DUDZ*: $\sigma_3' < 30$ kPa, *ODZ*: $30 \text{ kPa} < \sigma_3' < 75$ kPa, *CSDZ*: $\sigma_3' > 75$ kPa). The maximum deviator stress magnitude ($q_{max,cyc} = \sigma_{I' max} - \sigma_3'$) and static peak deviator stress ($q_{peak,sta}$) also plays an important role in characterising these degradation zones.

2.3 Ballast fouling

Ballast generally comprises of highly coarse-graded gravel-size particles, such as crushed or fractured rock or aggregates with sizes ranging from 10 mm to 63 mm and contains large void spaces. However, the infiltration of fouling materials reduces the void and restricts track drainage. The crushed rock fines (due to particle breakage), coal fines (due to spillage from coal wagons) and clay-silt fines (due to pumping of soft saturated subgrade) accumulate within the voids of the ballast bed and impair track drainage. For instance, excessive fouling due to coal and subgrade fines has lead to the formation of mud holes in the Goonyella System located in Central Queensland of Australia as shown in Figure 3. Several fouling indices are used in practice to measure the extent of ballast fouling. Selig and Waters (1994) have defined the fouling index as a summation of percentage (by weight) passing the 4.75 mm (No. 4) sieve and 0.075 mm (No. 200) sieve. They also proposed a percentage of fouling which is the ratio of the dry weight of fouled material passing through a 9.5 mm (3/8 inch) sieve to the dry weight of the total sample. These mass based indices give a false measurement of fouling when the fouling material has a different specific gravity. Feldman and Nissen (2002) defined the Percentage Void Contamination (*PVC*) as the ratio of bulk volume of fouling material to the volume of voids of clean ballast. However, this *PVC* does not consider the effect of the void ratio, gradation and specific gravity of the fouling material, which is the main factor affecting ballast drainage. Therefore, Void Contaminant Index (*VCI*) is proposed to incorporate these effects (Indraratna et al., 2010b):

$$VCI = \frac{(1 + e_f)}{e_b} \times \frac{G_{sb}}{G_{sf}} \times \frac{M_f}{M_b} \times 100 \quad (2)$$

where e_b is the void ratio of clean ballast, e_f is the void ratio of fouling material, G_{sb} is the specific gravity of the ballast material, G_{sf} is the specific gravity of the fouling material, M_b is the dry mass of clean ballast, and M_f is the dry mass of the fouling material.



Figure 3: Mudholes caused by excessive coal/clay fouling (Goonyella System, QR National: Photo courtesy of Michael Martin)

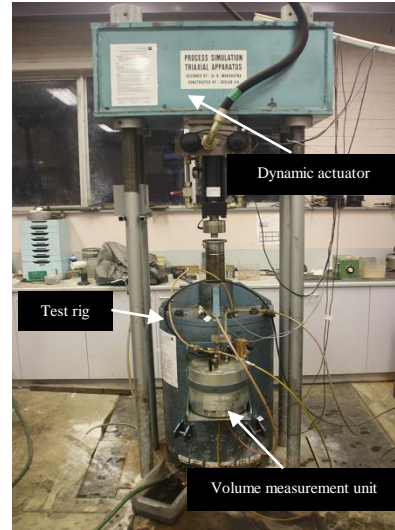


Figure 4: Large-scale cylindrical triaxial apparatus (Nimbalkar et al., 2012b)

In order to understand the effect of clay fouling on the stress-strain and degradation behaviour of railway ballast, for different levels of fouling, a series of monotonic triaxial tests were carried out for confining pressure in the range of 10-60 kPa. A large-scale cylindrical triaxial apparatus that could accommodate a specimen with height of 600 mm and diameter of 300 mm was designed and built at the University of Wollongong (Figure 4). The *PSD* of clean ballast used was as per recommended Australian Standards (AS 2758.7, 1996). Commercial kaolin was used to simulate clay fouling. Specific sample preparation techniques were employed for different levels of *VCI*. Details of these techniques and test setup can be found elsewhere (Indraratna et al., 2012). The sample was saturated by the application of back pressure of 80 kPa and the degree of saturation was assessed by employing the Skempton *B* test. When a *B* value of 0.98 was obtained (Skempton, 1954), the sample was judged to be sufficiently saturated. During testing, the required membrane correction was carried out according to ASTM D4767-04.

Figure 5 illustrates the deviator stress-strain response of clean ballast ($VCI = 0\%$) and clay-fouled ballast ($VCI = 10\%$ & 80%) at increasing confining pressure. When *VCI* increases, the peak deviator stress of clay-fouled ballast decreases significantly. At $VCI = 80\%$, clay fouled ballast shows an increasingly more ductile post-peak response. Figure 5 also shows the volumetric strain response for varying levels of fouling and increasing confining pressure. In the compression zone, the increasing *VCI* generally shows a reduced compression of the fouled specimen as the voids between the ballast grains are occupied by clay acting as void filler. Nevertheless, in the case of $VCI = 10\%$, an exception is observed for all three specimens (at $\sigma_3' = 10, 30, 60$ kPa) indicating a slightly increased compression compared to their fresh ballast counterparts. This may be attributed to the small amount of clay that is coating the ballast

grains as a lubricant, thereby facilitating the specimens to attain a slightly higher compression. In the dilation zone, the highly fouled specimens show a decrease in the rate and magnitude of dilation at axial strains exceeding @ 20%, while the increase in σ_3' from 10 to 60 kPa significantly suppresses dilation of all specimens. The addition of kaolin in sufficient quantities appears to contribute to a 'binding' effect that diminishes the tendency of the aggregates to dilate. Moreover, the specimens that are highly fouled ($VCI = 80\%$) begin to dilate swiftly at a lower axial strain after showing a reduced compression initially compared to clean ballast.

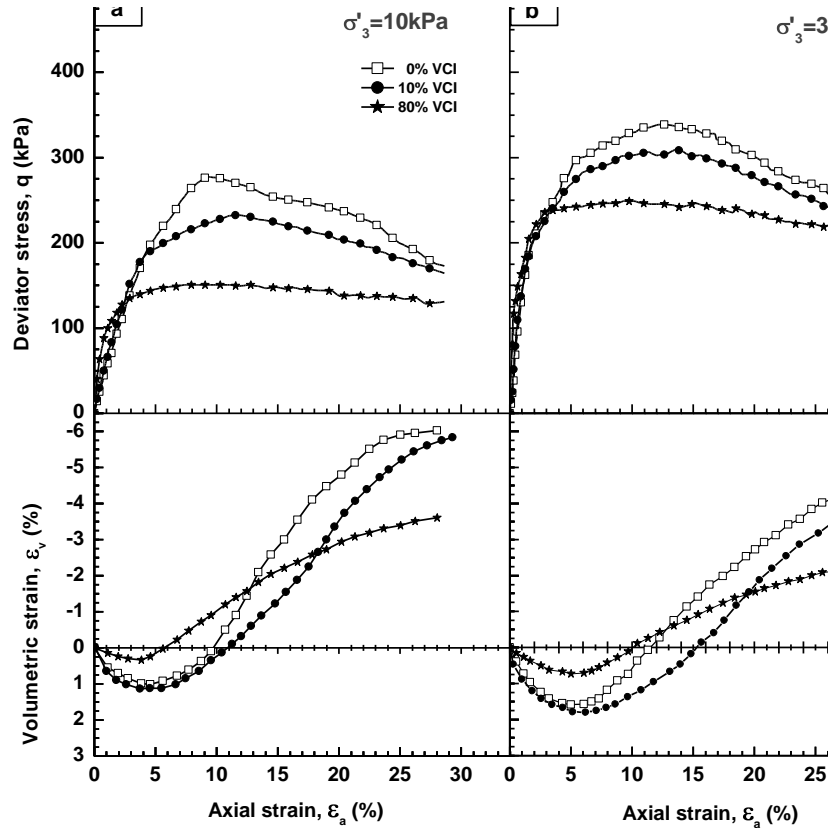


Figure 5: Stress-strain behaviour of clean and clay-fouled ballast at confining pressures (σ_3') of (a) 10 kPa, and (b) 30 kPa, respectively (data sourced from Tennakoon et al., 2012)

A shear strength envelope for clay-fouled ballast can be presented in a non-dimensional form as below:

$$\frac{\tau_f}{\sigma_c} = m \left(\frac{\sigma_n'}{\sigma_c} \right)^n \quad (3)$$

where τ_f , σ_n' and σ_c are shear stress, effective normal stress and uniaxial compressive strength of the parent rock. m and n are empirical coefficients and their values are obtained by best fit (regression) analysis using equations (4) and (5) respectively:

$$m = 0.07[1 + \tanh(VCI/21.5)] \quad (4)$$

$$n = 0.56[1 + 0.3\tanh(VCI/21.5)] \quad (5)$$

For a given ballast gradation, if the appropriate reduced peak deviator stress is not carefully selected on the basis of the anticipated fouling levels, this may over-predict the track bearing capacity and stability. Therefore, an accurate assessment of behaviour of clay-fouled ballast is highly beneficial for executing better maintenance schemes of existing tracks.

2.4 Use of shock mats for mitigating ballast breakage

A large scale drop-weight impact testing equipment was used to evaluate the effectiveness of shock mats in the attenuation of impact loads and subsequent mitigation of ballast breakage. The particle size distribution of ballast specimens was prepared in accordance with the current practice in Australia [AS 2758.7, 1996]. In order to resemble low track confining pressure in the field, the test specimens were confined in a rubber membrane (Figure 6a). A steel plate of 300 mm diameter and 50 mm thickness was used to represent a hard base such as the deck of a bridge, or hard rock. A 100 mm thick layer of compacted sand was used to simulate a typical 'weak' subgrade. Three layers of shock mat with a combined thickness of 30 mm were used. The drop hammer was raised mechanically to the required height and then released by an electronic quick release system. The impact load was stopped after 10 blows due to an attenuation of strains in the ballast layer.

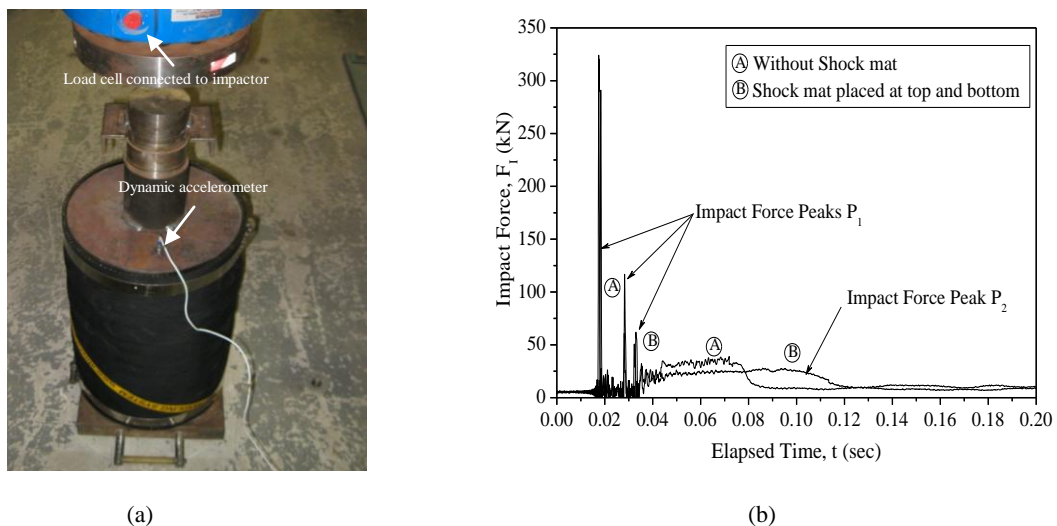


Figure 6: (a) Test Sample; (b) Typical impact force responses for stiff subgrade (data sourced from Nimbalkar et al., 2012a).

The impact load-time history under a single impact load is shown in Figure 6b. Two distinct types of peak forces were seen during impact loading, an instantaneous sharp peak with very high frequency, and a gradual peak of smaller magnitude with relatively lesser frequency.

Jenkins et al. (1974) termed these peak forces as P_1 and P_2 respectively. It was also evident that multiple P_1 type peaks followed by the distinct P_2 type peak often occurred. The multiple P_1 peaks occurred when the drop hammer was not restrained vertically, so that it rebounded after the first impact and hit the specimen again. The observed benefits of a shock mat are therefore twofold: (a) it attenuates the impact force and (b) it reduces the impulse frequencies thereby extending the time duration of impact. After each test, the ballast sample was sieved and breakage was obtained using *BBI* as shown in Table 1.

Table 1: Ballast breakage under impact loading (Indraratna et al., 2011a).

<i>Test No.</i>	<i>Base type</i>	<i>Test Details</i>	<i>BBI</i>
1	<i>Stiff</i>	<i>Without shock mat</i>	<i>0.170</i>
2	<i>Stiff</i>	<i>Shock mat at top and bottom of ballast</i>	<i>0.091</i>
3	<i>Weak</i>	<i>Without shock mat</i>	<i>0.080</i>
4	<i>Weak</i>	<i>Shock mat at top and bottom of ballast</i>	<i>0.028</i>

The higher breakage of ballast particles can be attributed to the considerable non-uniform stress concentrations occurring at the corners of the sharp angular particles of fresh ballast under high impact induced contact stresses. The impact from just 10 blows caused considerable breakage (i.e. *BBI* = 17%) when a stiff subgrade was used, but when a shock mat was placed above and below the ballast bed, particle breakage was reduced by approximately 47% for a stiff subgrade and approximately 65% for a weak subgrade. The weak subgrade itself acts as a flexible cushion.

3. From theory to practice: use of geosynthetics and mats

3.1 Field study at Bulli

In order to investigate train induced stresses, track deformations, and the benefits of using geosynthetics, a field trial was carried out on an instrumented track. The design specifications were provided by University of Wollongong, while the funding was contributed by RailCorp. Details of track construction and material specifications can be found in Indraratna et al., 2010a.

3.1.1 Track instrumentation

The performance of each section of track under the repeated loads of moving trains was monitored using sophisticated instrumentation. The vertical and horizontal stresses were measured by pressure cells. Vertical deformations of the track at different sections were measured by settlement pegs and lateral deformations were measured by electronic displacement transducers connected to a computer controlled data acquisition system. The

settlement pegs and displacement transducers were installed at the top and bottom of load bearing ballast layer, as shown in Figure 7.

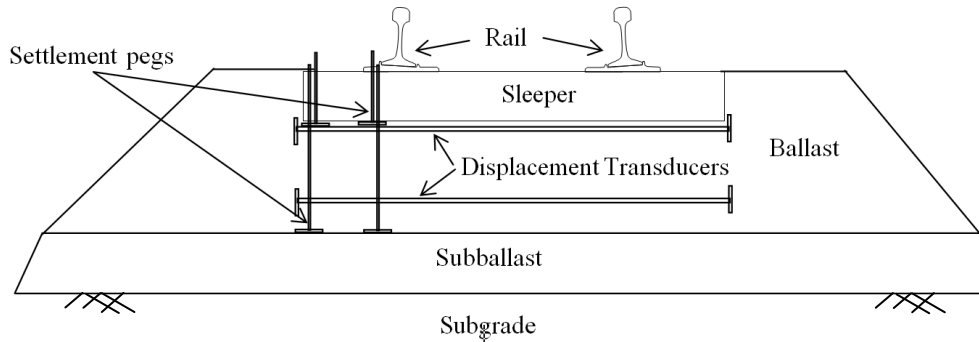


Figure 7: Installation of settlement pegs and displacement transducers at Bulli site

3.1.2 Track measurements: stresses and deformations

Figure 8(a) shows the maximum cyclic vertical (σ_v) and horizontal (σ_h) stresses recorded at Section 1 due to the passage of a coal train with 100-ton wagons (25 tons axle load). The stresses were measured under the rail and at the edge of the sleeper. It is evident that σ_v decreases significantly with depth, while σ_h decreases only marginally with depth. The large vertical stress and relatively small lateral (confining) stress caused large shear strains in the track.

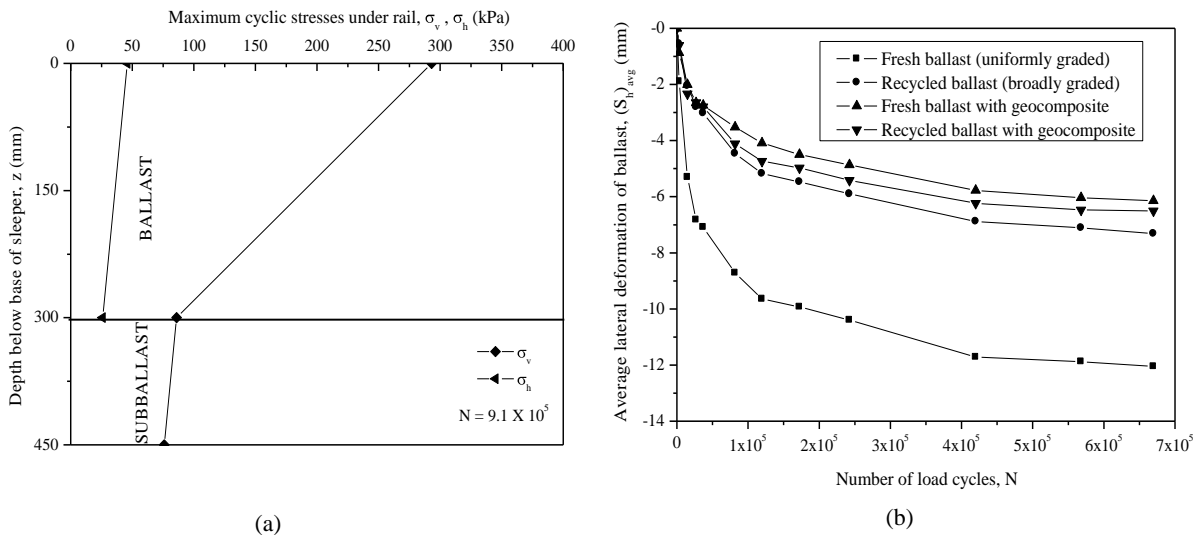


Figure 8: In-situ response of the ballast layer: (a) vertical stresses; (b) lateral deformations (data sourced from Indraratna et al., 2010a).

Average lateral deformations of ballast are plotted against the number of load cycles (N) in Figure 8(b). The recycled ballast showed less lateral deformations because of its moderately graded particle size distribution ($C_u = 1.8$) compared to the very uniform fresh ballast ($C_u =$

1.5). Recycled ballast often has less breakage because the individual particles are less angular which prevents corner breakage resulting from high contact stresses. The results presented in Figure 8b indicate that geocomposite reduced lateral deformation of fresh ballast by about 49 % and that of recycled ballast by 11 %. The apertures of the geogrid offered strong mechanical interlocking with the ballast. The capacity of the ballast to distribute loads was improved by the placement of the geocomposite layer, which substantially reduced settlement under high repeated loading.

3.2 Field study at Singleton

To investigate the performance of different types of geosynthetics to improve overall track stability under in situ conditions, an extensive study was undertaken on instrumented track sections near Singleton, NSW, which were part of the Third Track of the Minimbah Bank Stage 1 Line. The details of track construction and material specifications can be found in Indraratna et al., (2010a).

3.2.1 Track instrumentation

The strain gauges were installed in groups, 200 mm apart, and on the top and bottom sides of the grids in both longitudinal and transverse directions (Figure 9a). The strain gauges were a post yield type suitable to measure strains in the range of 0.1 to 15%. As shown in Figure 9b, two pressure cells were installed at Sections 1, 6, A and C. At these locations, one pressure cell was installed at the sleeper-ballast and another at the ballast-sub-ballast interface. At Section B however, three pressure cells were installed at the synthetic mat-deck interface. Settlement pegs were also installed at the sleeper-ballast and ballast-sub-ballast interfaces to measure vertical deformations of the ballast layer, as shown in Figure 9c.

3.2.2 Accumulated settlements of ballast layer

The settlements (S_v) and vertical strains (ε_v) of the ballast layer after 2.3×10^5 load cycles are reported in Table 2. The vertical settlements of sections with reinforcement are generally smaller than those without reinforcement. This phenomenon is mainly attributed to interlocking between the ballast particles and grids, thus creating larger track confinement. When Sections A, B, and C are compared, the results indicate that S_v and ε_v are larger when the subgrade stiffness becomes smaller, i.e. S_v are smallest on the concrete bridge deck and largest at the alluvial deposit.

It is also observed that geogrid is more effective in terms of reducing track settlement for softer subgrades. Similar observation was reported by Ashmawy and Bourdeau (1995) through full scale prototype testing. Geogrid at Section 4 performed better, although the tensile strength does not differ much with other types. This is attributed to optimum aperture size (40 mm) which would enable better interlocking between the ballast particles and geogrid.

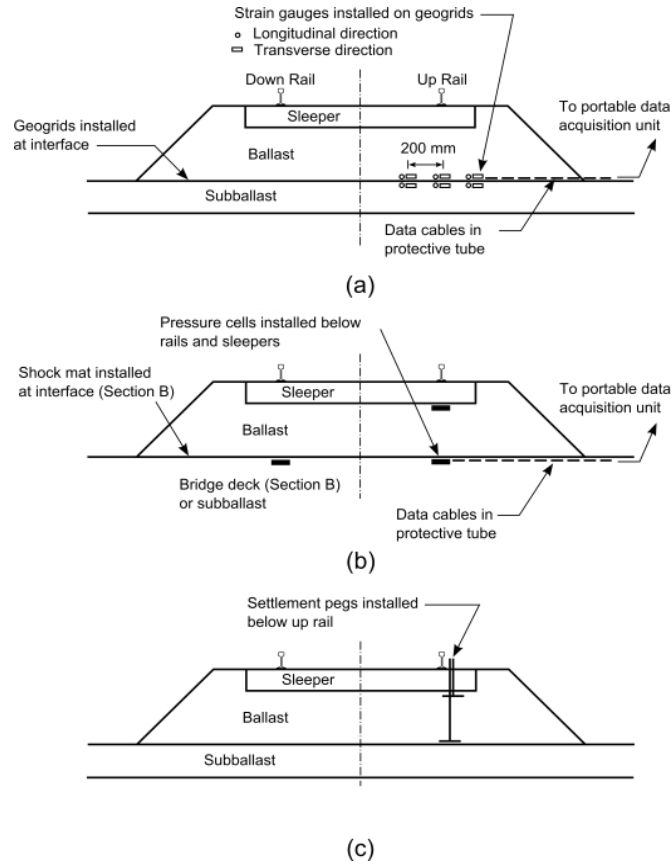


Figure 9: Details of track instrumentation using (a) strain gauges, (b) pressure cells and (c) settlement pegs.

Table 2: Vertical settlements and strains of ballast layer after 2.3×10^5 load cycles.

	Instrumented section details								
	1	2	3	4	5	6	A	B	C
Settlement S_v (mm)	16.3	21.2	20.6	14.8	16.0	16.3	23.8	8.8	17.8
Vertical strain ε_v (%)	5.4	7.1	6.9	4.9	5.3	5.4	7.9	2.9	5.9

3.2.3 Strains accumulated in geogrids

Accumulated longitudinal (ε_l) and transverse (ε_t) strains after 2.3×10^5 load cycles are given in Table 3. The transverse strains were generally larger than longitudinal strains, which is attributed to the relative ease for lateral spreading of the ballast. It was also observed that ε_l and ε_t are mainly influenced by deformations of the subgrade. The strains of geogrid at Section 5 were relatively large although its higher stiffness could have resulted in smaller strains. This is because the thick general fill underwent large lateral deformations shortly after the track was commissioned. Induced transient strains in both longitudinal and transverse directions due to the passage of trains (axial load of 30 tons) travelling at 40 km/h were of magnitude 0.14-0.17 %.

Table 3: Accumulated longitudinal and transverse strains in geogrid after 2.3×10^5 load cycles.

	<i>Instrumented section details</i>					
	<i>1</i>	<i>2</i>	<i>3</i>	<i>4</i>	<i>5</i>	<i>6</i>
<i>Longitudinal strain ε_l (%)</i>	<i>0.80</i>	<i>0.78</i>	<i>0.92</i>	<i>0.61</i>	<i>0.60</i>	<i>0.62</i>
<i>Transverse strain ε_t (%)</i>	<i>0.85</i>	<i>1.50</i>	<i>0.85</i>	<i>0.80</i>	<i>1.80</i>	<i>0.85</i>

4. Conclusions and recommendations

Effects of ballast fouling, geosynthetic reinforcement and shock mats on the performance of ballasted rail tracks are discussed in this keynote paper. The results highlight that particle breakage, confining pressure, ballast fouling in addition to loading patterns (cyclic and impact) have a significant influence on the engineering behaviour of ballast.

The detrimental effects of fouling on the shear strength characteristics were assessed using a new parameter, *VCI*. A series of isotropically consolidated drained monotonic triaxial tests using a large scale cylindrical triaxial apparatus were conducted on clay-fouled ballast. The shear strength envelope for clay-fouled ballast was expressed as a function of *VCI*. The use of shock mats was beneficial in terms of reduced ballast breakage and attenuated impact forces. Few impact blows caused the considerable ballast breakage ($BBI = 17\%$) in case of stiff subgrade. Due to placement of shock mat, *BBI* was reduced by approximately 47% using a stiff subgrade and by approximately 65% for a weak subgrade.

The performance of instrumented ballasted tracks at Bulli and Singleton was evaluated where different types of geosynthetics were used. The results of the Bulli field study indicated that the use of geocomposites as reinforcing elements for tracks using recycled ballast proved to be a feasible alternative. The results of the Singleton study revealed that the effectiveness of geogrids is more for relatively weak subgrade. The strains accumulated in geogrids were influenced by deformation of the subgrade, while the induced transient strains were mainly affected by the stiffness of geogrids. A better understanding of such a performance would allow for safer and more effective design and analysis of ballasted rail tracks with geosynthetic reinforcement and shock mats.

Acknowledgement

The Author wishes to thank the Australian Research Council, CRC for Rail Innovation, RailCorp, ARTC and Queensland Rail National for their continuous support. The financial support by CRC for Rail Innovation through grants R3.106 & R3.117 is gratefully acknowledged. A number of current and past PhD students, namely Dr Joanne Lackenby, Dr Wadud Salim, research fellow Miss Nayoma Tennakoon and Dr Pongpipat Anantanasakul have participated to the contents of this paper and their contributions are greatly acknowledged.

References

Altuhafi F and Coop M R (2011) "Changes to particle characteristics associated with the compression of sands." *Géotechnique* **61**(6): 459-471.

Ashmawy A K and Bourdeau P L (1995) "Geosynthetic-reinforced soils under repeated loading: a review and comparative design study." *Geosynthetics International* **2**(4): 643-678.

Feldman F and Nissen D (2002) "Alternative testing method for the measurement of ballast fouling: percentage void contamination." *Conference on Railway Engineering Wollongong, RTSA*, 101-109.

Indraratna B and Salim W (2003) "Deformation and degradation mechanics of recycled ballast-stabilised with geosynthetics." *Soils and Foundations* **43**(4): 35-46.

Indraratna B, Ionescu D and Christie D (1998) "Shear behaviour of railway ballast based on large-scale triaxial tests." *Journal of Geotechnical and Geoenvironmental Engineering ASCE* **124**(5): 439-439.

Indraratna B, Nimbalkar S, Christie D, Rujikiatkamjorn C and Vinod J S (2010a) "Field assessment of the performance of a ballasted rail track with and without geosynthetics." *Journal of Geotechnical and Geoenvironmental Engineering ASCE* **136**(7): 907-917.

Indraratna B, Salim W and Rujikiatkamjorn, C (2011a) *Advanced Rail Geotechnology – Ballasted Track* CRC Press/Balkema.

Indraratna B and Nimbalkar S (2012) "Stress-strain-degradation response of railway ballast stabilised with geosynthetics." *Journal of Geotechnical and Geoenvironmental Engineering ASCE* (accepted, in press).

Indraratna B, Lackenby J and Christie D (2005) "Effect of confining pressure on the degradation of ballast under cyclic loading." *Géotechnique* **55**(4): 325-328.

Indraratna B, Nimbalkar S and Tennakoon N (2010b) "The behaviour of ballasted track foundations: track drainage and geosynthetic reinforcement." *GeoFlorida 2010, ASCE Annual GI Conference*, February 20-24, 2010, West Palm Beach, Florida, USA: 2378-2387.

Indraratna B, Nimbalkar S, Rujikiatkamjorn C and Christie D (2011b) "State-of-the-art design aspects of ballasted rail tracks incorporating particle breakage, role of confining pressure and geosynthetic reinforcement." *Proceedings of 9th World Congress on Railway Research WCRR 2011*, Lille, France: 1-13.

Indraratna B, Tennakoon N, Nimbalkar S and Rujikiatkamjorn C (2012). "Behaviour of clay fouled ballast under drained triaxial testing." *Géotechnique* (accepted, in press).

Jenkins H M, Stephenson J E, Clayton G A, Morland J W and Lyon D (1974) "The effect of track and vehicle parameters on wheel/rail vertical dynamic forces." *Railway Engineering Journal* **3**: 2-16.

Lackenby J, Indraratna B, McDowel G and Christie D (2007) "Effect of confining pressure on ballast degradation and deformation under cyclic triaxial loading." *Géotechnique* **57**(6): 527-536.

Luo Y, Yin H and Hua C (1996) "Dynamic response of railway ballast to the action of trains moving at different speeds." *Proceedings of the Institution of Mechanical Engineers, Part F: Journal of Rail and Rapid Transit* **210**(2): 95-101.

Marsal R J (1973) *Mechanical properties of rock fill* In: Hirschfield R. C. and Pools, S. J. (eds) *Embankment Dam Engineering: Casagrande Volume*, Wiley, New York: 109-200.

Nimbalkar S, Indraratna B, Dash S K and Christie D (2012a) "Improved performance of railway ballast under impact loads using shock mats." *Journal of Geotechnical and Geoenvironmental Engineering ASCE* **138**(3): 281-294.

Nimbalkar S, Indraratna B, Rujikiatkamjorn C and Martin M (2012b) "Effect of coal fines on the shear strength and deformation characteristics of ballast." *Proceedings of the 11th Australia - New Zealand Conference on Geomechanics: Ground Engineering in a Changing World*, ANZ 2012, 15-18 July 2012, Melbourne, Australia: 451-456.

Raymond G P and Diyaljee V A (1979) "Railroad ballast load ranking classification." *Journal of Geotechnical Engineering ASCE* **105**(10): 1133-1153.

Raymond G P (2002) "Reinforced ballast behaviour subjected to repeated load." *Geotextiles and Geomembranes* **20**(1): 39-61.

Selig E T and Waters J M (1994) *Track Geotechnology and Substructure Management* Thomas Telford, London.

Skempton A W (1954) "The pore pressure coefficients A and B." *Géotechnique* **4**(4): 143-147.

Tennakoon N, Indraratna B, Nimbalkar S and Rujikiatkamjorn C (2012) "Deformation and degradation of clay fouled ballast subjected to monotonic loading." *Proceedings of the International Conference on Ground Improvement and Ground Control ICGI 2012*, 30 Oct.-2 Nov. 2012, University of Wollongong, Australia (accepted, in press).

Tutumluer E, Dombrow W and Huang H (2008) "Laboratory characterization of coal dust fouled ballast." *Proceedings of the AREMA 2008 Annual Conference and Exposition*, 21-24 September 2008, Salt Lake City, Utah. American Railway Engineering and Maintenance-of-Way Association, Lanham: 93-101.